International Journal of Mycobacteriology 5 (2016) 197–204

Available at www.sciencedirect.com
ScienceDirect
journal homepage: www.elsevier.com/locate/IJMYCO

Limonia acidissima L. leaf mediated synthesis of zinc oxide nanoparticles: A potent tool against *Mycobacterium tuberculosis*

Bheemanagouda N. Patil, Tarikere C. Taranath *

Postgraduate Department of Studies in Botany, Environmental Biology Laboratory, Karnatak University, Dharwad, Karnataka, India

ARTICLE INFO

Article history:
Received 28 February 2016
Accepted 5 March 2016
Available online 31 March 2016

Keywords:
Limonia acidissima L.
MABA
Mycobacterium tuberculosis
Mycolic acid
Zinc oxide nanoparticles

ABSTRACT

Objective/background: The present investigation was undertaken to synthesize zinc oxide nanoparticles using *Limonia acidissima* L. and to test their efficacy against the growth of *Mycobacterium tuberculosis*.

Methods: The formation of zinc oxide nanoparticles was confirmed with UV–visible spectrophotometry. Fourier transform infrared spectroscopy shows the presence of biomolecules involved in the stabilization of zinc oxide nanoparticles. The shape and size was confirmed with atomic force microscope, X-ray diffraction, and high resolution transmission electron microscope. These nanoparticles were tested for their effect on the growth of *M. tuberculosis* through the microplate alamar blue assay technique.

Results: The UV–visible data reveal that an absorbance peak at 374 nm confirms formation of zinc oxide nanoparticles and they are spherical in shape with sizes between 12 nm and 53 nm. These nanoparticles control the growth of *M. tuberculosis* at 12.5 μg/mL.

Conclusion: Phytosynthesis of zinc oxide nanoparticles is a green, eco-friendly technology because it is inexpensive and pollution free. In the present investigation, based on our results we conclude that the aqueous extract of leaves of *L. acidissima* can be used for the synthesis of zinc oxide nanoparticles. These nanoparticles control the growth of *M. tuberculosis* and this was confirmed with the microplate alamar blue method. The potential of biogenic zinc oxide nanoparticles may be harnessed as a novel medicine ingredient to combat tuberculosis disease.

Introduction

In modern science, the entire biological field has been using nanotechnology within a short amount of time. This era of nanotechnology helps in the production of materials at the smallest possible scale. Nanotechnology has considerably improved and revolutionized plenty of technologies that are used in industrial sectors including food safety, medicine, and other fields. Zinc oxide nanoparticles are used in the generation of biological applications including semiconducting, piezoelectric, and pyroelectric properties, and have versatile applications in transparent electronics, UV light emitters,

* Correspondence to: Prof. Tarikere C. Taranath, Environmental Biology Laboratory, Post Graduate Department of Botany, Pavate Nagar Karnatak University, Dharwad 580003, Karnataka, India. Mobile: +91 9480335735, +91 9986935735.
E-mail address: tctaranath@rediffmail.com (T.C. Taranath).

Peer review under responsibility of Asian African Society for Mycobacteriology.
http://dx.doi.org/10.1016/j.ijmyco.2016.03.004

personal care products, and coating and paints [1,2]. Zinc oxide nanoparticles with various sizes and shapes have been widely exploited in numerous technological applications as biosensors in medical diagnostics [3]. Zinc oxide nanoparticles have also been proposed as antimicrobial preservatives for wood and food products [4,5]. Nanoparticles enhance the immobilization and activity of catalysts in the pharmaceutical industry [6,7], gas sensors [7], antimicrobial activity [8] electronic nanodevices, and UV filters [9] due to the novel properties exhibited by the material. For all these requirements of nanoparticles different methods are developed via physical, chemical, and biological methods; however, these physicochemical methods [10] generate large amounts of hazardous by-products. Biological methods are simple, eco-friendly reaction protocols for the synthesis of nanoparticles by using plant extracts that provide a biological synthesis route of several metallic nanoparticles which are more eco-friendly and allows capping, reduction, and control with well-defined size and shape. The bio-fabrication of zinc nanoparticles by *Justicia adhatoda* leaf extract [11] and *Aloe barbadensis* leaf extract are used to synthesize zinc oxide nanoparticles [12], gold nanoparticles are synthesized by using plants such as lemon grass and neem [13,14], and *Limonia acidissima* leaf extract has been used for the synthesis of silver nanoparticles [15]. Zinc oxide as a nontoxic, inexpensive, and nonhygroscopic polar inorganic crystalline material is very economical, safe, and easily available Lewis acid catalyst, which has gained much interest in various organic transformations, sensors, transparent conductors, and surface acoustic-wave devices [16–18].

Tuberculosis (TB) continues to be one of the leading causes of death worldwide. The World Health Organization declared TB as a global emergency in 1993. According to a recent World Health Organization report, there were 1.5 million TB-related deaths in 2014. TB is the world's second most common cause of death after human immunodeficiency virus/AIDS. The presence of immunosuppressive factors like diabetes, alcoholism, malnutrition, chronic lung disease, and human immunodeficiency virus/AIDS may increase the chances of TB infection [19,20]. The disease affects the lungs mainly, but can also develop as pulmonary TB in the central nervous system, circulatory system, or elsewhere in the body [21].

Available TB treatment involves daily administration of four oral antibiotics for a period of $\geqslant$6 months [22]. Due to a high percentage of side effects (ototoxicity and nephrotoxicity) and the extended duration of treatment results in low patient adherence [23]. Based on this concept the field of nanotechnology focuses on the preparation of TB diagnostic kits which are currently under trial. This technology does not require any skill and is cost effective. Another significant advancement of this technology is that the use of nanoparticles as drug carriers has high stability and carrier capacity. Today, different types of nanoparticles are used to control the growth of *Mycobacterium tuberculosis* viz the alginate nanoparticles help the bioadhesive characteristics of intestinal mucosa therapy which increases the time period available for its absorption [24]. Chitosan, rifampicin, and polyethylene glycol nanoparticles are used in the controlled delivery system for TB treatment [25]. Banu and Rathod [26] used biogenic silver nanoparticles to inhibit the growth of *M. tuberculosis* [26]. The decoction of *L. acidissima* leaves are used for the treatment of constipation, vomiting, and also as a cardiotonic and diuretic in Indian folk medicine [27]. The leaves are reported to possess hepatoprotective activity [28]. Leaves, bark, and fruits of this plant have been used in traditional medicine for centuries due to their antimicrobial [29], antifungal [30], astringent, anti-inflammatory [31], and insulin secretagogue [32] activities. Essential oil isolated from the leaves has antibacterial and antifungal activity [33]. In view of all these aspects, the present investigation was undertaken to bio-fabricate zinc oxide nanoparticles using *L. acidissima* leaf extract and to test their efficacy against TB bacterial growth.

Materials and methods

L. acidissima Linn. Syn. *Feronia elephantum* Correa, (wood apple) is a medicinally important plant (Fig. 1A and B). It is a moderate sized deciduous tree grown throughout India. Dark greenish fresh leaves of wood apple without any infection were sampled from the botanical garden at Karnatak University, Dharwad Karnataka, India, and zinc nitrate (Hi-media, Mumbai, India) was used for the biosynthesis of zinc oxide nanoparticles.

Preparation of the plant extract

Twenty grams of fresh leaves were washed with tap water followed by Milli-Q water and then were dried, finely cut, and soaked in a 250-mL Erlenmeyer flask containing 100-mL Milli-Q water and boiled at 60 °C for 1 h. The leaf extract was allowed to cool at room temperature, filtered through Whatman number-1 filter paper, and the filtrate was stored at 4 °C for further experimental use.

Fig. 1 – (A) *Limonia acidissima* L. leaves; (B) habitat of the plant.

Biosynthesis and characterization of zinc oxide nanoparticles

Five milliliters of the extract was added to a 95-mL zinc nitrate solution in a 250-mL Erlenmeyer flask, and incubated at 80 °C for 10 min. The pH was adjusted to 10 using 0.1 N HCl or 0.1 N NaOH. Reduction of zinc ions to zinc nanoparticles was observed after 72 h. The leaf extract and zinc nitrate were maintained as controls throughout the experimental period.

Characterization was done with a UV–visible spectrophotometer (Jasco Corporation, Tokyo, Japan) at a resolution of 1 nm, with a wavelength range of 300–600 nm. The solution was centrifuged (Remi R-8C) at 4500 g for 40 minutes, and pellets were redispersed in Milli-Q water. The centrifugation and dispersion were repeated to ensure the removal of excess biomolecules. The purified pellets were dried in an oven, subjected to the fourier transform infrared spectroscopy with the help of KBr pellets, and recorded the spectrum (U-3010 spectrophotometer) at a resolution of 4 nm with a range of 400–4000 cm^{-1}. Particle size and distribution of the nanoparticles were determined using an atomic-force microscopy (AFM) and high-resolution transmission electron microscopy (HR-TEM) model of Tap190Al-G of nanosurf easy scan2 and JEOL 3010, respectively. An energy-dispersive X-ray spectrometer was used for analysis (EDAX-TSL Ametek).

Anti-TB activity using microplate alamar blue dye assay method

The anti-TB activity of zinc oxide nanoparticles was assessed against *M. tuberculosis* (H37 RV strain) American Type Culture Collection No-27294 using a standard microplate alamar blue dye assay method [34]. This method is nontoxic, employs a thermally stable reagent, and shows good correlation with proportional and BACTEC radiometric methods. Two-hundred microliters of sterile deionized water was added to all outer perimeter wells of a sterile 96 well plate to minimize evaporation of the medium from the test wells during incubation. The 96 wells of the plate received 100 μL of Middlebrook 7H9 broth and a serial dilution of zinc oxide nanoparticles were made directly on the plate. The final zinc oxide nanoparticle concentrations tested were 0.8–100 μg/mL, and standard antibiotics like pyrazinamide, ciprofloxacin, and streptomycin were used. Plates were covered and sealed with parafilm and incubated at 37 °C for 5 days. After incubation, 25 μL of the freshly prepared 1:1 mixture of alamar blue reagent and 10% Tween 80 was added to the plate and incubated for 24 h. A blue color in the well was considered as no bacterial growth, and the pink color was scored as growth. The minimum inhibitory concentration was defined as the lowest drug concentration which prevented the color change from blue to pink.

Results and discussion

The biological approaches for the synthesis of zinc oxide nanoparticles using *L. acidissima* leaf extract at 80 °C for a 10-min duration for the reduction of zinc nitrate to zinc oxide nanoparticles by bioreduction, stabilizing, and capping with

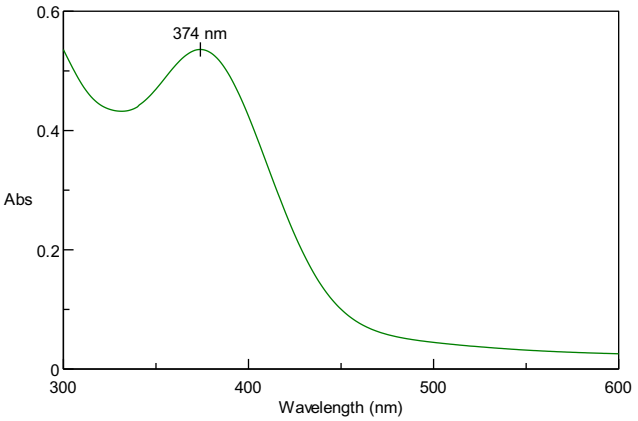

Fig. 2 – UV–visible spectrum of zinc oxide nanoparticles synthesized by leaf extract of *Limonia acidissima*. Note. Abs = absorbance.

leaf extract, has a peak at 374 nm in the UV–visible spectra data (Fig. 2) which this is very similar to the synthesis of zinc oxide nanoparticles by *Parthenium* leaf extract [8].

Fig. 3 and Table 1 shows the Fourier transform infrared spectroscopy spectrum recorded from the zinc oxide nanoparticles obtained after oven drying of the centrifuged fine powder. The amino acid residue and the peptide of protein presents the well-known signature in the infrared region of the electromagnetic spectrum. The phenol molecules are present at 3412 cm^{-1} stretching vibration, and the 1610-cm^{-1} band reveals the carboxylate group. The peak at 1056 cm^{-1} was assigned to the Si–O–Si stretching vibration of proteins while their weak bending vibrations of 1268 cm^{-1} was assigned to the carbonyl stretching vibration of guaiacyl ring. The 1409-cm^{-1} band represents the C–C stretching of the aromatic ring. The infrared study reveals the presence of aromatic ring proteins and amide bonds have a strong ability for the formation and covering of metal nanoparticles. The characteristic absorption peak of the zinc oxide bond was found to be 543 cm^{-1} [35,36].

Fig. 4 shows the strong signals of zinc and oxygen atoms in the nanoparticles recorded in the energy dispersive X-ray analysis, and other signals from C, Mg, Ca, and Si atoms were also observed.

The morphology and size of nanoparticles were ascertained from the AFM and HR-TEM images. AFM data reveal that the particles are monodispersed and spherical in shape and that the size ranges from 12 nm to 53 nm (Fig. 5A) in two- and three-dimensional structures of the nanoparticles with a height of 14.4 nm (Fig. 5B). The distance from each other is 11.3–56.52 nm (Fig. 5C). The particles are spherical in shape and some of the particles are agglomerates. The HR-TEM image confirms the formation of zinc oxide nanoparticles and they have an average size of about 12–53 nm (Figs. 5 and 6). The obtained zinc oxide nanoparticles are similar to that of *A. barbadensis* [12].

XRD was performed to further confirm the action of the zinc oxide phase of the nanoparticles. The XRD of the obtained nanoparticles is shown in Fig. 7. The XRD peaks were identified as (100), (002), (101), (102), (110), and (112)

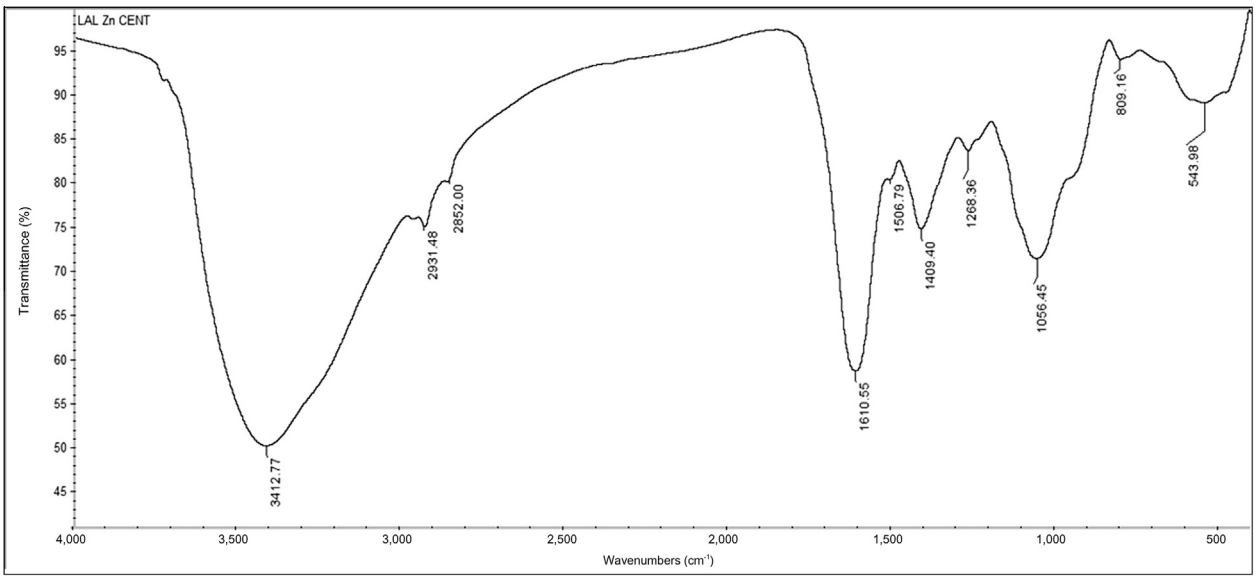

Fig. 3 – Fourier transform infrared spectroscopy spectrum of biogenic zinc oxide nanoparticles.

Table 1 – Fourier transform infrared spectroscopy absorption peaks and their associated functional groups involved in the biosynthesis of zinc oxide nanoparticles.

Serial no.	Absorption peak (cm^{-1}) in zinc oxide nanoparticles	Bond/functional groups
1	543.98	Stretching of hydroxyl group
2	809.16	Waging of secondary amines
3	1056.45	Si–O–Si stretching vibration of proteins
4	1268.36	C–O stretching vibration of guaiacyl ring
5	1409.40	C–C stretching of aromatic ring
6	1506.79	N–O asymmetric stretching of nitro compounds
7	1610.55	C=C stretching of vinyl alkyl ethers
8	2852.00	C–CH_2 groups in chitosan or oleic acid
9	2931.48	C–H stretching vibrations of alkanes
10	3412.77	O–H stretching vibrations of phenol group

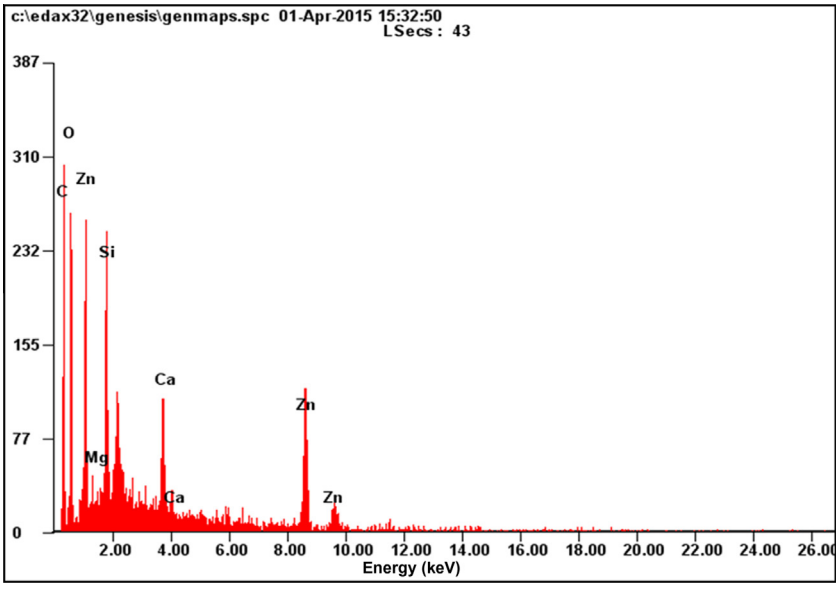

Fig. 4 – Energy-dispersive X-ray spectrometer spectrum of zinc oxide nanoparticles.

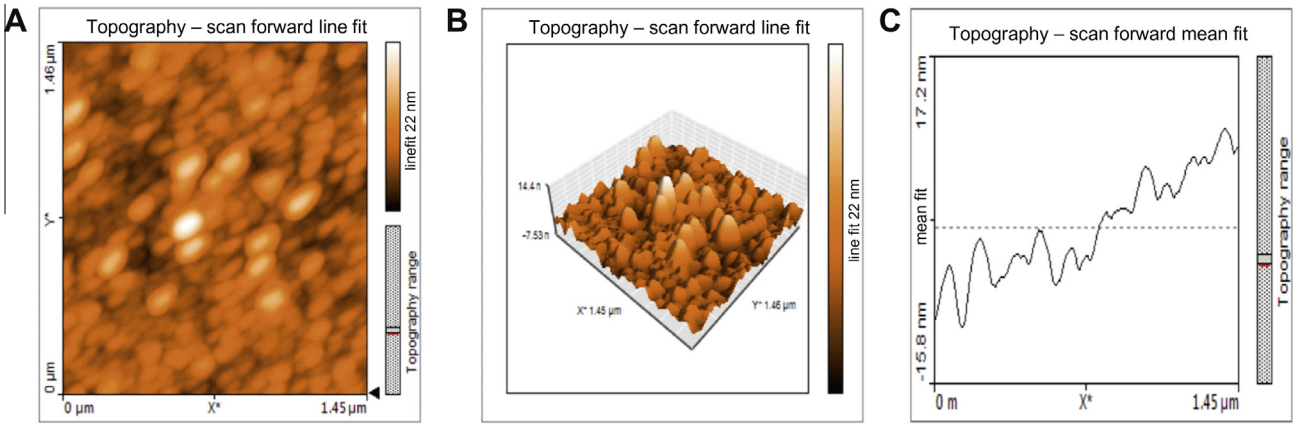

Fig. 5 – (A) Two-dimensional structure; (B) three-dimensional image; (C) particle size distribution of zinc nanoparticles.

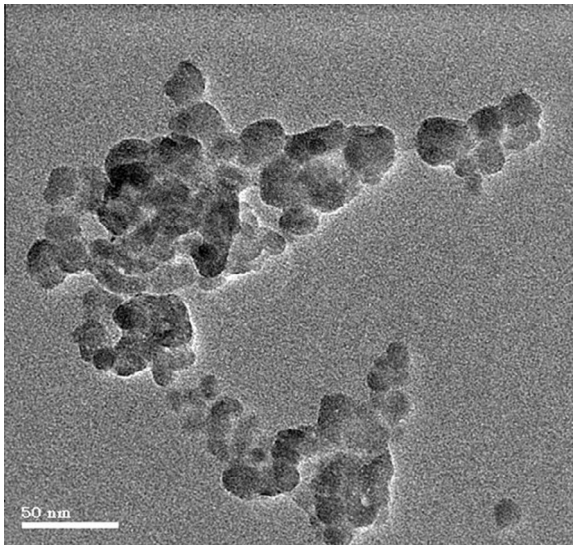

Fig. 6 – High-resolution transmission electron microscopy image of zinc oxide nanoparticles.

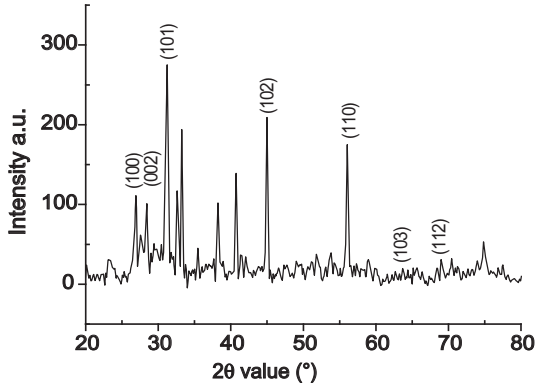

Fig. 7 – X-ray powder diffraction spectrum of zinc oxide nanoparticles with Bragg's diffraction values shown in parentheses. The absorbance is expressed in terms of arbitrary unit (a.u.).

reflections, respectively. All of the diffraction peaks can be indexed to the spherical and hexagonal zinc oxide phase by comparison with the data from Joint Committee on Powder Diffraction Standards card number 89-7102. The narrow and strong diffraction peaks indicate that the product has a well defined crystalline particle structure. The Scherrer formula was used for the calculation of the particles sizes and found to be in the range of 12–53 nm.

Effect of zinc oxide nanoparticles on M. tuberculosis

Reports from assays on the toxicity of zinc oxide nanoparticles on the *M. tuberculosis* system are meager. However, there are few reports on the toxic effects of alginate nanoparticles which possess bioadhesive characteristics to intestinal mucosa therapy which increases the time period available for its absorption [24]. Chitosan, rifampicin, and polyethylene glycol nanoparticles are used in controlled delivery systems for TB treatment [25]. Banu and Rathod [26] used the biogenic silver nanoparticles to inhibit the growth of *M. tuberculosis* [26]. Table 2 and Fig. 1 shows the inhibition of *M. tuberculosis* growth after being treated with zinc oxide nanoparticle solution. The bacteria were exposed to different concentrations (0.8 µg/mL, 1.6 µg/mL, 3.12 µg/mL, 6.25 µg/mL, 12.5 µg/mL, 25 µg/mL, 50 µg/mL, and 100 µg/mL) of zinc oxide nanoparticle solution and showed the bacterial sensitivity with increasing concentrations of solution exposed to the *M. tuberculosis*. Zinc nanoparticles after completion of the incubation period showed a blue color in the well which is considered as no bacterial growth, and pink color is scored as a growth. Bacterial growth was inhibited from 12.5 µg/mL to 100 µg/mL of zinc oxide nanoparticles. However, at a concentration of 12.5 µg/mL the zinc oxide nanoparticles have a minimum inhibitory concentration or modest effect on bacterial growth. The mycobacterium were sensitive at 100 µg/mL of leaf extract but resistant to zinc nitrate solution in all concentrations (Fig. 8 and Table 2). Standard antibiotics like pyrazinamide and ciprofloxacin shows the minimum inhibitory concentration at 3.12 µg/mL but streptomycin shows 6.25 µg/mL.

The current investigation suggests that the biologically synthesized zinc oxide nanoparticles from a medicinal plant

Table 2 – Shows the results of antituberculosis activity.

Samples name	Concentration (μg/mL)							
	100	50	25	12.5	6.25	3.12	1.6	0.8
ZnO NPs	S	S	S	S	R	R	R	R
Zinc nitrate	R	R	R	R	R	R	R	R
Leaf extract	S	R	R	R	R	R	R	R
Pyrazinamide	S	S	S	S	S	S	R	R
Ciprofloxacin	S	S	S	S	S	S	R	R
Streptomycin	S	S	S	S	S	R	R	R

Note. NPs = nanoparticles; R = resistant; S = sensitive.

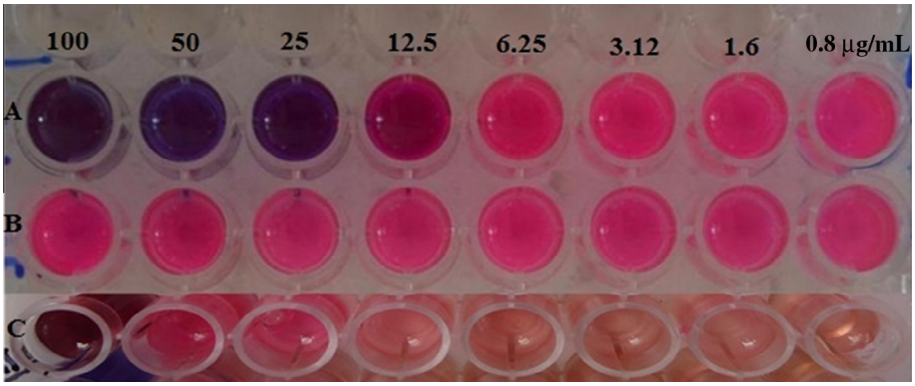

Fig. 8 – Microplatealamar blue assay method was used to determine the minimum inhibitory concentrations of biogenic zinc oxide nanoparticles against *Mycobacterium tuberculosis*: (A) biogenic zinc nanoparticles; (B) zinc nitrate; (C) leaf extract.

can be used as a better alternative antimicrobial drug for the treatment of infectious diseases caused by pathogenic microorganisms.

There are meager reports on the activity of zinc oxide nanoparticles on *M. tuberculosis*. Although zinc oxide nanoparticles can be internalized into bacteria, less or no genotoxic potential has been reported in *Salmonella typhimurium* and *Escherichia coli* [37,38]. In Fig. 8A, 100 μg/mL, 50 μg/mL, 25 μg/mL, and 12.5 μg/mL of zinc oxide nanoparticle solution inhibited the growth of bacteria where the zinc oxide nanoparticles initiate a lipid peroxidation reaction subsequently causing DNA damage, glutathione depletion, disruption of membrane morphology, and electron transport chain, which leads to cell apoptosis [39]. The concentration and size (12–53 nm) are two important factors that may affect cell apoptosis. In Fig. 9, the zinc oxide nanoparticles are found to be attached on the surface of the bacterial cell membrane. After that it enters into the cytoplasm of mycobacterium via endocytosis and the smaller sized nanoparticles (12–53 nm) penetrate the bacterial cell membrane which inactivates the enzymes essential for adenosine triphosphate production [7,40] that leads to the formation of reactive oxygen species

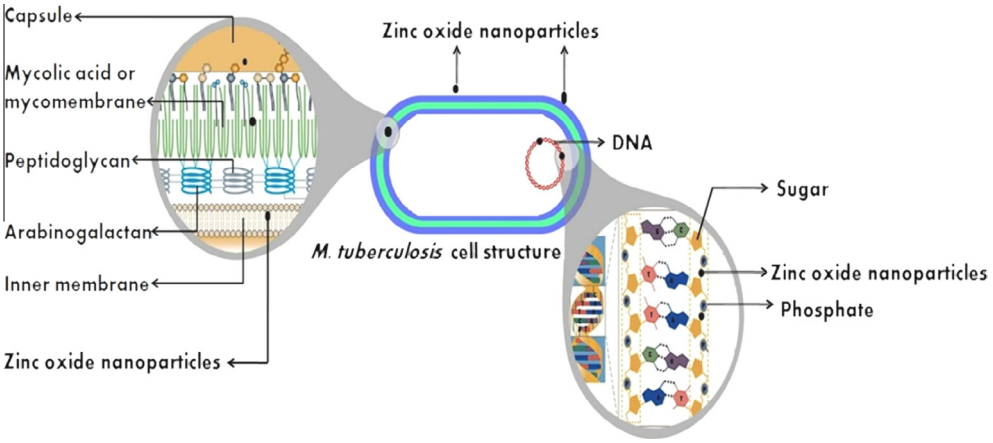

Fig. 9 – Schematic diagram depicting the possible mechanism of activity of zinc oxide nanoparticles on *Mycobacterium tuberculosis*.

and eventually bacterial cell apoptosis [41]. The zinc oxide nanoparticles may react with sulfur or phosphorus-containing soft bases, such as R-S-R, R-SH, RS-, or PR3, and it promotes the loss of DNA replication ability [42–44]. Thus, the sulfur-containing protein in the membrane or inside the cell and phosphorus-containing elements like DNA are likely to be preferential sites for the action of zinc oxide nanoparticles [44].

The inhibition depletes the sites of mycolic acid transfer to the cell wall. Mycolic acids present in cell walls are known to be specifically attached to the 5-position of distal D-arabinose residue as shown by Azuma and Yamamura [45]. The depletion of newly synthesized mycolic acids must find alternative sites for transfer. This transfer is thought to be diverted to the trehalose molecule, which causes overproduction of trehalose monomycolate and trehalose dimycolate. This effect of ethambutol may trigger a cascade of changes in the lipid metabolism of *Mycobacterium smegmatis* and *M. tuberculosis* leading to cell damage and eventually to cell apoptosis [46–48]. Zinc oxide nanoparticles may bring about bacterial cell apoptosis as with ethambutol. Fig. 9 shows the schematic representation of the possible mechanism of activity of zinc oxide nanoparticles on *M. tuberculosis*.

Conclusion

This investigation demonstrates that zinc oxide nanoparticles can be synthesized through a green approach that is an inexpensive, pollution free, and eco-friendly method using *L. acidissima* leaf extract as a bio-templating agent. The biogenic zinc oxide nanoparticles are spherical in shape and ranges from 12 nm to 53 nm. Based on this observation, an interaction between zinc oxide nanoparticles and the cell surface affects the permeability of the membrane where nanoparticles enter and induce the generation of reactive oxygen species in the bacterial cell, subsequently resulting in the inhibition of cell growth and eventually resulting in cell death.

Conflicts of interest

The authors have no conflicts of interest.

Acknowledgments

The authors thank the Chairman of the Postgraduate Department of Studies in Botany, Karnatak University, Dharwad, India, for providing the necessary facilities. B.N.P. acknowledges the financial support in the form of a UGC–UPE: University Grant Commission–University with Potential for Excellence fellowship (reference number KU/Sch/UGC-UPE/2013-14/1101) and the UGC–DSA–I: University Grant Commission–Departmental Special Assistance–I phase program of the Department of Botany, Karnatak University, Dharwad Campus. The authors also thank USIC: University Scientific Instrumentation Centre, K.U. Dharwad, STIC: Sophisticated Test and Instrumentation Centre, Kochin, SRM University, and DST: Department of Science and Technology Nano unit, IITM: Indian Institute of Technology Madras, Chennai for providing the necessary instrumentation facility.

REFERENCES

[1] Z.L. Wang, Nanostructures of zinc oxide, Mater. Today 7 (2004) 26–33.
[2] M.S. Akhtar, S. Ameen, S.A. Ansari, et al, Synthesis and characterization of ZnO nanorods and balls nanomaterials for dye sensitized solar cells, J. Nanoeng. Nanomanuf. 1 (2011) 71–76.
[3] Z. Zhang, H. Chen, J. Zhong, et al, Nanotip-based QCM biosensors, in: Proceedings of the IEEE International Frequency Control Symposium and Exposition, 2006, pp. 545–549.
[4] V. Aruoja, H. Dubourguier, C. Kasamet, et al, Toxicity of nanoparticles of CuO, ZnO and TiO_2 to microalgae *Pseudokirchneriella subcapitata*, Sci. Total Environ. 407 (2009) 1461–1468.
[5] C.A. Clausen, S.N. Kartal, R.A. Arango, et al, The role of particle size of particulate nano-zinc oxide wood preservatives on termite mortality and leach resistance, Nanoscale Res. Lett. 6 (2011) 427.
[6] P. Wang, Nanoscale biocatalyst systems, Curr. Opin. Biotechnol. 17 (2006) 574–579.
[7] B. Baruwati, D.K. Kumar, S.V. Manorama, Hydrothermal synthesis of highly crystalline ZnO nanoparticles: a competitive sensor for LPG and EtOH, Sens. Actuators B Chem. 119 (2006) 676–682.
[8] P. Rajiv, S. Rajeshwari, R. Venckatesh, Bio-fabrication of zinc oxide nanoparticles using leaf extract of *Parthenium hysterophorus* L. and its size-dependent antifungal activity against plant fungal pathogens, Spectrochim. Acta A Mol. Biomol. Spectrosc. 112 (2013) 384–387.
[9] S. Singh, P. Thiyagarajan, K.M. Kant, et al, Structure, microstructure and physical properties of ZnO based materials in various forms: bulk, thin film and nano, J. Phys. D Appl. Phys. 40 (2007) 6312–6327.
[10] M. Li, H. Bala, X. Lv, et al, Direct synthesis of monodispersed ZnO nanoparticles in an aqueous solution, Mater. Lett. 61 (2007) 690–693.
[11] T.C. Taranath, N.P. Bheemanagouda, T.U. Santosh, et al, Cytotoxicity of zinc nanoparticles fabricated by *Justicia adhatoda* L. on root tips of *Allium cepa* L.—a model approach, Environ. Sci. Pollut. Res. 22 (2015) 8611–8617.
[12] G. Sangeetha, S. Rajeshwari, R. Venckatesh, Green synthesis of zinc oxide nanoparticles by *Aloe barbadensis* miller leaf extract: structure and optical properties, Mater. Res. Bull. 12 (2011) 2560–2566.
[13] S.S. Shankar, A. Rai, A. Ahmad, et al, Controlling the optical properties of lemongrass extract synthesized gold nanotriangles and potential application in infrared-absorbing optical coatings, Chem. Mater. 17 (3) (2005) 566–572.
[14] S.S. Shankar, A. Rai, A. Ahmad, et al, Rapid synthesis of Au, Ag, and bimetallic Au core–Ag shell nanoparticles using neem (*Azadirachta indica*) leaf broth, J. Colloid Interface Sci. 275 (2004) 496–502.
[15] N.P. Bheemanagouda, T.C. Taranath, Antituberculosis activity of biogenic silver nanoparticles synthesized by using aqueous leaf extract of *Limonia acidissima* L., Int. J. Pharm. BioSci. 7 (2016) 89–97.
[16] K. Bahrami, M.M. Khodaei, A. Nejati, One-pot synthesis of 1,2,4,5-tetrasubstituted and 2,4,5-trisubstituted imidazoles

by zinc oxide as efficient and reusable catalyst, Monatsh. Chem. 142 (2011) 159–162.
[17] R. Tayebee, F. Cheravi, M. Mirzaee, et al, Commercial zinc Oxide (Zn_2^+) as an efficient and environmentally benign catalyst for homogeneous benzoylation of hydroxyl functional groups, Chin. J. Chem. 28 (2010) 1247–1252.
[18] C.R. Gorla, N. Emanetoglu, W.S. Liang, et al, Structural, optical, and surface acoustic wave properties of epitaxial ZnO films grown on (01–12) sapphire by metalorganic chemical vapor deposition, J. Appl. Phys. 85 (1999) 2595–2602.
[19] B.J. Marais, K. Lonnroth, S.D. Lawn, et al, Tuberculosis comorbidity with communicable and non-communicable diseases: integrating health services and control efforts, Lancet Infect. Dis. 13 (2013) 436–448.
[20] I.G. Sia, M.L. Wieland, Current concepts in the management of tuberculosis, Mayo Clin. Proc. 86 (2011) 348–361.
[21] R.B. Rock, M. Olin, C.A. Baker, et al, Central nervous system tuberculosis: pathogenesis and clinical aspects, Clin. Microbiol. Rev. 21 (2008) 243–261.
[22] L.C. du Toit, V. Pillay, M.P. Danckwerts, Tuberculosis chemotherapy: current drug delivery approaches, Respir. Res. 7 (2006) 118.
[23] C. Aagaard, J. Dietrich, M. Doherty, et al, TB vaccines: current status and future perspectives, Immunol. Cell Biol. 87 (2009) 279–286.
[24] Z. Ahmad, R. Pandey, S. Sharma, et al, Alginate nanoparticles as antituberculosis drug carriers: formulation development, pharmacokinetics and therapeutic potential, Indian J. Chest Dis. Allied Sci. 48 (2006) 171–176.
[25] M. Rajan, V. Raj, Encapsulation, characterization and in-vitro release of anti-tuberculosis drug using chitosan-poly ethylene glycol nanoparticles, Int. J. Pharm. Pharm. Sci. 4 (2012) 255–259.
[26] A. Banu, V. Rathod, Biosynthesis of monodispersed silver nanoparticles and their activity against *Mycobacterium tuberculosis*, J. Nanomed. Biother. Discov. 3 (2013) 1–5.
[27] T.K. Chatterjee, Herbal Options, third ed., Books and Allied (P) Ltd., Calcutta, 2000, pp. 203–256.
[28] C.D. Kamat, K.R. Khandelwal, S.L. Bodhankar, et al, Hepatoprotective activity of leaves of *Feronia elephantum* Correa (Rutaceae) against carbon tetrachloride induced liver damage in rats, J. Nat. Remedies 3 (2003) 148–154.
[29] B.M.R. Bandara, C.M. Hewage, D.H.L.W. Jayamanne, et al, Biological activity of some steam distillates from leaves of ten species of rutaceous plants, J. Nat. Sci. Counc. 18 (1990) 71–77.
[30] N.K.B. Adikaram, Y. Abhayawardhane, A.A.L. Gunatilaka, et al, Antifungal activity, acid and sugar content in the wood apple (*Limonia acidissima*) and their relation to fungal development, Plant Pathol. 38 (2007) 258–265.
[31] K.H. Kim, S.K. Ha, S.Y. Kim, et al, Limodissimin A: a new dimeric coumarin from *Limonia acidissima*, Bull. Korean Chem. Soc. 30 (2009) 2135–2137.
[32] R. Gupta, S. Johri, A.M. Saxena, Effect of ethanolic extract of *Feronia elephantum* Correa fruits on blood glucose level in normal and streptozotocin-induced diabetic rats, Nat. Prod. Rad. 8 (2009) 32–33.
[33] R.K. Joshi, V.M. Badakar, S.D. Kolkute, et al, Chemical composition and antimicrobial activity of the essential oil of the leaves of *Feronia elephantum* (Rutaceae) from north west Karnataka, Nat. Prod. Commun. 6 (2011) 141–143.
[34] M.C.S. Lourenço, M.V.N. de Souza, A.C. Pinheiro, et al, Evaluation of anti-tubercular activity of nicotinic and isoniazid analogues, Arkivoc (2007) 181–191.
[35] K. Nejati, Z. Rezvani, R. Pakizevand, Synthesis of ZnO nanoparticles and investigation of the ionic template effect on their size and shape, Int. Nano Lett. 1 (2011) 75–81.
[36] H. Kumar, R. Rani, Structural and optical characterization of ZnO nanoparticles synthesized by microemulsion route international letters of chemistry, Int. Lett. Chem. Phys. Astron. 14 (2013) 26–36.
[37] A. Kumar, A.K. Pandey, S.S. Singh, et al, Cellular uptake and mutagenic potential of metal oxide nanoparticles in bacterial cells, Chemosphere 83 (2011) 1124–1132.
[38] S.H. Nam, S.W. Kim, Y.J. An, No evidence of the genotoxic potential of gold, silver, Zinc oxide and titanium dioxide nanoparticles in the SOS chromotest, J. Appl. Toxicol. 33 (2013) 1061–1069.
[39] A. Kumar, A.K. Pandey, S.S. Singh, et al, Engineered ZnO and TiO_2 nanoparticles induce oxidative stress and DNA damage leading to reduced viability of *Escherichia coli*, Free Radic. Biol. Med. 51 (2011) 1872–1888.
[40] Q.L. Feng, J. Wu, G.Q. Chen, et al, A mechanistic study of the antibacterial effect of silver ions on *Escherichia coli* and *Staphylococcus aureus*, J. Biomed. Mater. Res. 52 (2000) 662–668.
[41] S. Mohanty, P. Jena, R. Mehta, et al, Antimicrobial peptides and biogenic silver nanoparticles kill mycobacterium without eliciting DNA damage and cytotoxicity in mouse macrophages, Antimicrob. Agents Chemother. 57 (2013) 3688–3698.
[42] M. Yamanaka, K. Hara, J. Kudo, Bactericidal actions of a silver ion solution on *Escherichia coli* studied by energy-filtering transmission electron microscopy and proteomic analysis, Appl. Environ. Microbiol. 71 (2005) 7589–7593.
[43] A. Kumar, P.K. Vemula, P.M. Ajayan, et al, Silver-nanoparticle embedded antimicrobial paints based on vegetable oil, Nat. Mater. 7 (2008) 236–241.
[44] K.R. Raghupathi, R.T. Koodali, A.C. Manna, Size-dependent bacterial growth inhibition and mechanism of antibacterial activity of zinc oxide nanoparticles, Langmuir 27 (2011) 4020–4028.
[45] I. Azuma, Y. Yamamura, Studies on the firmly bound lipids of human tubercle bacillus. II. Isolation of arabinose mycolate and identification of its chemical structure, J. Biochem. 53 (1963) 275–278.
[46] K. Takayama, E.L. Armstrong, Metabolic role of free mycolic acids in *Mycobacterium tuberculosis*, J. Bacteriol. 130 (1977) 569–570.
[47] J.O. Kilburn, J. Greenberg, Effect of ethambutol on the viable cell count in *Mycobacterium smegmatis*, Antimicrob. Agents Chemother. 11 (1977) 534–540.
[48] K. Takayama, E.L. Armstrong, K.A. Kunugi, et al, Inhibition by ethambutol of mycolic acid transfer into the cell wall of *Mycobacterium smegmatis*, Antimicrob. Agents Chemother. 16 (1979) 240–242.